Burns & Trauma, 2021, 9, tkab021
https://doi.org/10.1093/burnst/tkab021
Research Article

Research Article

Curcumin preconditioning enhances the efficacy of adipose-derived mesenchymal stem cells to accelerate healing of burn wounds

Maryam Azam[1], Hafiz Ghufran[1], Hira Butt[1], Azra Mehmood[1], Ramla Ashfaq[1], Asad M. Ilyas[1], Muhammad R. Ahmad[1] and Sheikh Riazuddin[1,2,*]

[1]National Centre of Excellence in Molecular Biology, 87-West Canal Bank Road, University of the Punjab, Lahore, Pakistan and [2]Jinnah Burn and Reconstructive Surgery Centre, Maulana Shaukat Ali Rd, Quaid-i-Azam Campus, Lahore, Pakistan

*Correspondence. Email: riazuddin@aimrc.org

Received 5 January 2021; Revised 26 March 2021; Editorial decision 28 April 2021

Abstract

Background: Following recent findings from our group that curcumin preconditioning augments the therapeutic efficacy of adipose-derived stem cells in the healing of diabetic wounds in rats, we aimed to investigate the regenerative effects of curcumin preconditioned adipose-derived mesenchymal stem cells (ASCs) for better recovery of acid inflicted burns in this study.

Methods: ASCs were preconditioned with 5 μM curcumin for 24 hours and assessed for proliferation, migration, paracrine release potential and gene expression comparative to naïve ASCs. Subsequently, the healing capacity of curcumin preconditioned ASCs (Cur-ASCs) versus naïve ASCs was examined using acidic wounds in rats. For this, acid inflicted burns of 20 mm in diameter were made on the back of male Wistar rats. Then, 2×10^6 cells of Cur-ASCs and naïve ASCs were intradermally injected in the wound periphery ($n = 6$) for comparison with an untreated saline control. Post-transplantation, wounds were macroscopically analysed and photographed to evaluate the percentage of wound closure and period of re-epithelization. Healed wound biopsies were excised and used for histological evaluation and expression analysis of wound healing markers at molecular level by quantitative PCR and western blotting.

Results: We found that Cur-ASCs exhibited greater proliferation, migration and paracrine potential *in vitro*. Further, Cur-ASCs showed more effective recovery than naïve ASCs as exhibited by gross morphology, faster wound closure and earlier re-epithelialization. Masson's trichrome and hematoxylin and eosin staining demonstrated the improved architecture of the healing burns, as evidenced by reduced infiltration of inflammatory cells, compact collagen and marked granulation in Cur-ASC treated rats. Corroborating these findings, molecular assessment showed significantly reduced expressions of pro-inflammatory factors (interleukin-1 beta, interleukin-6, tumor necrosis factor alpha) a with striking upsurge of an oxidative marker (superoxide dismutase 1), pro-angiogenic factors (vascular endothelial growth factor, hepatocyte growth factor, hypoxia-inducible factor-1 alpha) and collagen markers (transforming growth factor beta 1, fibroblast growth factor-2, collagen type 1 alpha 1), verifying that Cur-ASCs modulate the regulation of pro-inflammatory and healing markers at burn sites.

Conclusions: Treatment with Cur-ASCs resulted in faster re-epithelization of acid inflicted burns compared to the treatment with naïve ASCs. Based on observed findings, we suggest the

transplantation of Cur-ASCs is a valuable therapy for the potent clinical management of acidic burns.

Key words: Adipose-derived stem cells, Curcumin preconditioning, Acidic burn, Wound healing

Highlights

- Curcumin preconditioning augments the therapeutic efficacy of ASCs by increasing their metabolic and migratory potential and paracrine release ability.
- Cur-ASCs are superior to naïve ASCs in terms of hastening the re-epithelialization and closure of acidic burn wounds.
- Subcutaneous administration of Cur-ASCs around wound edges accelerates healing by suppressing inflammation, enhancing antioxidant and angiogenic responses and improving collagen deposition.

Background

The incidence of burn injuries caused by fire, electricity, radiation and chemicals is growing worldwide with substantial risk of morbidity and mortality. According to a World Health Organization report, more than 11 million cases of burns require medical attention annually, including 1–5 million victims of chemical injuries, of which 30% confronting death [1,2]. In addition to this high mortality, patients who recover often suffer permanent post-burn scarring and disfigurement that leads to psychological disturbance, social isolation and rejection from society [3]. Current management strategies for burns include standard of care treatment, with either temporary application of hydrocolloid dressings following early excision, or use of the gold-standard technique, which involves treating the burns by harvesting split thickness skin grafts from unburned areas. However, these methods have limitations in cases where patients have few unburned areas remaining [4]. This emphasizes the need for effective treatments and advanced interventions in order to improve survival and quality of life for patients suffering from acid-induced burns [5].

Over the past years, mesenchymal stem cell (MSC)-based reconstruction has emerged as a robust means by which to repair damaged skin [6–8]. Among MSCs, adipose-derived MSCs (ASCs) in particular have practical advantages owing to their non-invasive acquisition, high yield and remarkable *ex vivo* proliferative potential [9]. In addition, ASCs secrete numerous regenerative factors, such as vascular endothelial growth factor (VEGF), basic fibroblast growth factor, hepatocyte growth factor (HGF) and stromal cell-derived factor-1 [10]. Thus, they are considered to be promising cellular candidates for wound repair therapy in the field of regenerative medicine [11,12]. Furthermore, in this context, a number of animal studies have demonstrated the effective healing ability of ASCs in various hard-to-heal chronic wounds and suggested the mechanism of action is the secretion of growth factors that drive rapid re-epithelialization and enhance granulation and neovascularization [13–16]. However, inflammation-associated oxidative stress at the wound site ferociously affects the survival of engrafted ASCs, thus limiting their predicted therapeutic outcomes [17]. Hence, pre-induction of cytoprotective stimuli in the ASCs, thereby promoting their survival in the harsh microenvironment, is supposed to be an important strategic advancement in regenerative medicine.

Several adjunctive strategies have been explored recently, including genetic modification and priming (also referred to as preconditioning), in order to further enhance the therapeutic potential of transplanted MSCs. Existing priming approaches involve pre-incubation with pharmacological/-chemical agents, trophic factors/cytokines and a hypoxic condition [18,19]. For example, Srifa *et al.* reported that MSCs genetically engineered to hypersecrete Platelet-derived growth factor-BB (PDGF-BB) and Vascular endothelial growth factor A (VEGF-A) accelerate wound healing in a diabetic mouse model after implantation [20]. Ariyanti *et al.* demonstrated that salidroside pretreatment improved MSC survival, antioxidant defense and migration potential under hyperglycemia and, ultimately, promoted wound healing in diabetic mice model [21]. These studies showed that modified MSCs have superior therapeutic effects compared with wild type MSCs. However, relative to other cell modification approaches, pretreatment seems more feasible and reproducible from the perspective of clinical application.

Curcumin, an active constituent of turmeric (*Curcuma longa*), possesses potent antioxidant, anti-inflammatory and anti-tumorigenic traits and has been reported to exert cytoprotective effects against oxidative and inflammatory stresses in several cell studies [22–27]. Recent reports have shown that curcumin can protect ASCs from oxidative stress-induced injury via a heme oxygenase-1 dependent mechanism [28,29]. In another study, it has been demonstrated that curcumin can reverse the detrimental effects of oxidative stress on osteogenic differentiation of ASCs [30]. Moreover, we recently reported that curcumin preconditioning maintained the therapeutic potential of ASCs against hyperglycemic stress *in vitro* and healed diabetic wounds promptly upon transplantation *in vivo* [31]. Hence, in this study, we

hypothesized that curcumin preconditioned ASCs (Cur-ASCs) can be more effective compared with naïve ASCs for accelerating healing of acid burns.

Therefore, in present study, we locally injected the Cur-ASCs into acid burns in rat model and evaluated their regenerative efficacy by analysing injury recovery rate and regulation of key healing markers at the molecular level.

Methods

Experimental animals

Twenty-two male Wistar rats were used for the isolation and culturing of adipose-derived stem cells (n = 4) and the *in vivo* study (n = 18). This research and all experimental procedures were approved by the institution review board of the National Centre of Excellence in Molecular Biology, University of the Punjab, Lahore, Pakistan.

Culturing of ASCs

ASCs from rat adipose tissue were isolated by following a previously reported protocol [32]. Briefly, 2–4 g adipose was collected from the abdomen of the rats and washed with phosphate buffered saline (PBS) followed by manual mincing with a sterile surgical blade. Minced adipose was subjected to enzymatic digestion in collagenase-1 solution (1 mg/ml) (Sigma Aldrich, USA) for 45 minutes at 37°C. Then, the enzyme was inactivated by Dulbecco's Modified Eagle Medium (DMEM-LG) (Sigma Aldrich, USA) containing 15% fetal bovine serum (FBS) (Sigma Aldrich, USA). Subsequently, isolated ASCs were cultured in DMEM-LG supplemented with 15% FBS and 1% antibiotic solution (100 IU penicillin and 100 µg/ml streptomycin) (Sigma Aldrich, USA). Fresh medium was added on every third day. ASCs were used at passage 3 (P3) for further experiments.

Characterization of ASCs

ASCs with and without curcumin preconditioning were analysed for the presence of MSC markers (cluster of differentiation (CD) 90, CD105) and absence of hematopoietic (CD45) and endothelial (CD34) markers by immunocytochemistry. In brief, cells were fixed with 2% paraformaldehyde (Sigma Aldrich, USA) followed by blocking of non-specific bindings with 5% bovine serum albumin for 30 minutes and overnight incubation with primary antibodies, i.e anti-CD34, anti-CD45, anti-CD90 and anti-CD105 (1:50; Santa Cruz, USA) at 4°C. After primary incubation cells were washed twice with PBS and incubated with corresponding Alexa Fluor labeled secondary antibodies (1:700; Invitrogen, USA) for 1 hour at 37°C. Nuclei counterstaining was performed with 4, 6-diamidino-2-phenylindole (Invitrogen, USA). Twenty images were captured randomly using a BX61 fluorescent microscope (Olympus, Japan) for further analysis.

Furthermore, naïve ASCs and Cur-ASCs were checked for their differentiation potential into adipocytes, chondrocytes and osteocytes using StemPro® Differentiation Kits. Cells were plated in 12-well cell culture plates (4×10^3 cells/well) by following the standard kit protocols. All 3 differentiation media were prepared by following the guidelines in the manufacturers' data sheets. Non-induced controls in each assay were maintained in a serum-free medium for the same period.

Adipogenic differentiation was confirmed after 7 days. Differentiated cells were fixed with 10% formalin (Sigma Aldrich, USA) for 15 minutes. After fixation, cells were washed and stained with 0.5% oil red O (Sigma Aldrich, USA) for 10 minutes. Oil red O is a fat-soluble dye that strongly stains lipids and neutral triglycerides in frozen sections and lipid droplets and oily vesicles in differentiated adipocytes. After 10 minutes of staining, cells were washed with distilled water and images were captured using an IX51 light microscope (Olympus, Japan).

Chondrogenic differentiation was confirmed after 14 days by Alcian blue 8GX (Sigma-Aldrich, USA), which is used to stain glycosaminoglycans (acidic polysaccharides) in cartilage and to prove the ability of chondrogenic cells to secrete proteoglycans. After 14 days, cells were fixed, washed and stained (15 minutes) with filtered 1% Alcian blue solution prepared in 0.1 M HCl. Then, the cells were washed with distilled water to neutralize the acidity. Images were obtained using an IX51 light microscope.

Osteogenic differentiation was confirmed after 21 days by Alizarin red S stain (Sigma Aldrich, USA), which is used to assess mineralization in osteogenic differentiated cells. Osteogenic differentiation was confirmed after 21 days by Alizarin red S stain (Sigma Aldrich, USA). This stain form complexes with calcium deposits of osteocytes by chelation process. For this, differentiated cells were fixed, washed and incubated with 2% Alizarin red S for 3 minutes. Following incubation, cells were washed with PBS and images were obtained using an IX51 microscope.

Curcumin preconditioning of ASCs

Preconditioning of ASCs was achieved by following the same dosage and strategy as previously reported [31]. In brief, cells were incubated in a medium (serum-free DMEM-LG) containing 5 µM curcumin obtained from *C. longa* (Sigma-Aldrich, USA; >65% pure) for 24 hours and used as Cur-ASCs. Cells incubated in a curcumin-free medium were used as non-preconditioned ASCs.

Cell proliferation assay

The proliferation capacity of ASCs with and without curcumin preconditioning was assessed by MTT assay. ASCs were seeded in 96-well plates (1.5×10^4 cells/well) and exposed to curcumin preconditioning medium for 24 hours as previously described. After 24 hours, the preconditioning medium was replaced with 15% DMEM-LG and cells were assessed in terms of their proliferation at day 1, day 4 and day 7. At each time point, cells were treated with 5 mg/ml MTT solution (Sigma Aldrich, USA) for 3 hours and the formed formazan crystals were resuspended in dimethyl

sulfoxide. Then, absorbance was recorded at 570 nm with a reference wavelength at 650 nm using a spectrophotometer (Spectrostar Nano, BMG Labtech, USA).

In vitro cell migration assay

To determine the cell migration potential of Cur-ASCs compared with non-preconditioned ASCs, an *in vitro* wound healing scratch assay was performed. For this, cells were seeded in 6-well plates (1×10^6 cells/well). After 70–80% confluency, cells were subjected to curcumin preconditioning and then a scratch was made in the middle of each well with a micropipette (P200) tip. After 12 hours, filling of scratched empty spaces was observed under microscopy, images were taken and *in vitro* wound reduction was calculated using ImageJ software (National Institutes of Health, USA).

Enzyme-linked immunosorbent assay

The paracrine release potential of both non-preconditioned ASCs and Cur-ASCs was analysed using enzyme-linked immunosorbent assay (ELISA). For this, primary antibodies, (Abcam, USA) including epidermal growth factor (1:1000), VEGF (1:500) and fibroblast growth factor (1:500), and their respective secondary antibodies, were used. The concentration of each paracrine factor was calculated in pg/ml.

Acid burn injury model and ASC transplantation

Injury was induced in male Wistar rats aged 3–4 months and weighing 200–250 g. Rats were anesthetized with ketamine (100 mg/kg) and xylazine (10 mg/kg) and their backs shaved with an electric hair trimmer (Dingling professional hair clipper, RF-608, Dingling, China). A sterile filter paper disc 20 mm diameter was soaked in 12.06 N HCl (Merck, USA) for 1 minute and applied at the dorsal side of the neck for 10 minutes to inflict the acid burn injury (Figure 1a). Post-burn, analgesia was given for pain relief to all rats by subcutaneous administration of buprenorphine (0.05 mg/kg). Twenty-four hours after the injury, necrotic tissue was carefully removed and rats were randomly divided into following groups (n = 6 for each group) based on the treatment approach: (1) control (saline injected), (2) ASCs (non-preconditioned ASCs injected) or (3) Cur-ASCs (Cur-ASCs injected). Post-burn, excised necrotic tissue was fixed in 10% formalin solution, paraffin processed and subjected to hematoxylin and eosin (H&E) staining for injury characterization. Images were captured using an IX51 microscope, assessed by an experienced pathologist for burn depth measurement and compared with normal skin to articulate the severity and extent of the injury (Figure 1b). On the transplantation day, 1 ml cell suspension was injected intradermally (2×10^6 cells/wound) around the wound perimeter at a volume of 0.25 ml (250 µl) per quadrant (Figure 1c). Likewise, 1 ml saline was injected into the wounds of control rats. After transplantation wounds were dressed carefully with Mepore bandages (Mepore, Sweden).

Wound assessment and biopsies collection

Wound healing was assessed by analysing the percentage of wound closure. For this, wounds were photographed on days 4, 8, 12, 16 and 20 post-transplantation. The percentage of wound closure was calculated using the following formula [33]:

$$\%\text{of wound closure} = \frac{\text{wound area on day 0} - \text{open wound area}}{\text{wound area on day 0}} \times 100\%$$

On complete healing, rats were sacrificed to collect healed skin biopsies from the transplantation site. Excised tissue was instantly divided into 3 pieces. One part was preserved in a 10% formalin buffer (Sigma-Aldrich, USA) for histology; one in RNAlater, an RNA stabilization reagent (Qiagen, USA), for mRNA expression analysis; and one in a radio-immunoprecipitation assay buffer (Sigma-Aldrich, USA) with protease inhibitor (Calbiochem, USA) for protein expression analysis (Figure 1c).

Histological evaluation

Following paraffin processing, fixed tissues were cut (5 µm thick) using a HM-340E microtome (Microm Inc., USA) and subjected to Masson's trichrome and H&E staining. Briefly, for collagen content assessment sections were stained with Masson's trichrome (Sigma Aldrich, USA) as per the manufacturer's protocol and, for evaluation of skin architecture, stained with H&E according to standard protocol and then mounted with Cytoseal 60 (Richard Allen Scientific, USA). Images were captured using an IX51 microscope and evaluated via digital scoring by a certified pathologist blinded to the experiment. Ten ×40 power fields were randomly selected from each group by using an IX51 microscope and evaluated via digital scoring by a certified pathologist blinded to the experiment. Following scoring method was used: inflammatory cells permeation (0 = none, 1 = minimal, 2 = mild, 3 = severe); extent of collagen deposition (0 = none, 1 = minimal, 2 = mild, 3 = abundant); and granulation content (0 = none, 1 = minimal, 2 = mild, 3 = evident) [31, 34].

Quantitative RT-PCR and western blotting for key healing markers

To evaluate the effect of curcumin preconditioning on ASCs and the wound recovery rate at the molecular level, mRNA expression of different healing markers was assessed by qRT-PCR. In brief, RNA was extracted from both curcumin preconditioned and non-preconditioned cells (*in vitro* cell culture experiments) and from collected healed skin (*in vivo* animal experiments) using Trizol reagent (Sigma-Aldrich, USA) and cDNA was synthesized using a cDNA synthesis kit (Invitrogen, USA). Then, Maxima Syber Green master mix (Fermentas, USA) was used to perform qRT-PCR and reactions were run on a Pikoreal96 Real time-PCR system (Thermo Scientific, USA). Primers with sequences are provided in Table 1. β-actin was used for normalization and relative mRNA was analysed by Quantification cycle (Cq) values.

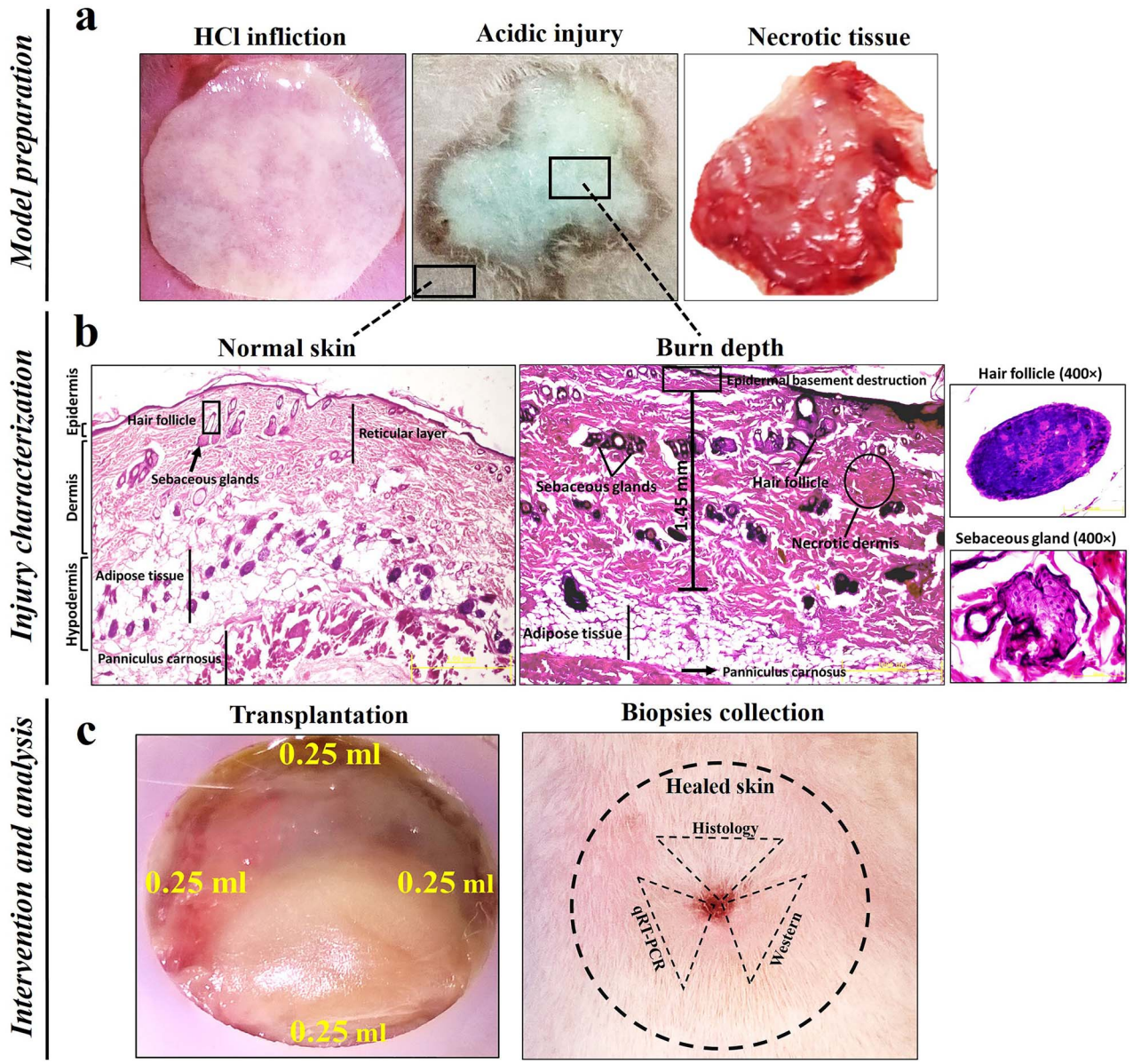

Figure 1. Schematic illustration of acidic burn model preparation, injury characterization, cell intervention and analysis of excised healed tissue. **(a)** Model preparation: a 2 × 2 cm sterile filter paper disc was soaked in 12.06 N HCl (for 1 minute) and placed on the hair-free back of experimental rats (for 10 minutes) for acid exposure to the skin. Acid exposure produced skin burns and ultimately necrotic tissue upon penetration. **(b)** Injury characterization: 24 hours after injury, microscopic assessment of hematoxylin and eosin stained sections of normal and burned skin (×40) was performed for measurement of burn depth and severity. Normal skin histology showed that all layers were intact and viable; in burned skin, acid penetration resulted in a deep partial thickness second degree burn (1.45 mm in depth) with epidermal basement destruction, damage to the dermal reticular layer and necrotic collagen with intact dermal adnexa (i.e. sebaceous gland, hair follicle) and hypodermis. **(c)** Intervention and analysis: after excision of necrotic tissue, a suspension of adipose-derived mesenchymal stem cells (2×10^6) prepared in phosphate buffered saline (1 ml) was injected into the wounds. Cells were transplanted intradermally around the wound periphery with 0.25 ml (250 µl) delivered to each quadrant as written in yellow. At the time of sacrifice, the healed area of the skin was traced by drawing the 2×2 cm^2 circle with marker as shown in black and sections from the central portion were collected for post-healing analysis as illustrated by the dotted black triangles

Protein expressions were analysed using western blotting. For this, protein was extracted and quantified by Bio-Rad protein assay dye (Bio-Rad, USA). Then, sodium dodecyl sulphate–polyacrylamide gel electrophoresis (SDS-PAGE) was performed for weight-based separation of proteins (30 µg from each skin sample). Separated proteins were transferred (blotted) on nitrocellulose membranes (Amersham Biosciences, UK) that were subsequently incubated with the respective primary and secondary antibodies (Table 2). Last, protein bands were visualized by applying chromogenic substrates (Sigma-Aldrich, USA) i.e. 3,3-diaminobenzidine/3,3,5,5 tetra methylbenzidine for horseradish peroxidase conjugated antibody and 5-bromo-4-chloro-3-indolyl phosphate/nitro blue tetrazolium for

Table 1. List of primers used in the study

Gene	Forward primer	Reverse primer
IL-1β	CCAAGCACCTTCTTTTCCTTC	AGACAGCACGAGGCATTTT
IL-6	CCACCCACAGACCAGTA	CTCCAGAAGACCAGAGCAGAT
TNF-α	TGCCTCAGCCTCTTCTCATT	GCTTGTGGTTTGCTACGAC
SOD1	TGCTTTTTGCTCTCCCAGGT	CTGGACCGCCATGTTTCTTA
TGF-β1	TGCGCCTGCAGAGATTCAAG	AGGTAACGCCAGGAATTGTTGCT
FGF-2	GTATGTGGCACTGAAACGAAC	TCAGCTCTTAGCAGACATTGG
COL1α1	CAAGATGGTGGCCGTTACTAC	TTAGTCCTTACCGCTCTTCCAG
HGF	ATGAGAGAGGCGAGGAGAAAC	GTAGCCCCAGCCGTAAATACT
HIF1-α	CCCATCCATGTGACCATGAG	AATCAGCACCAAGCACGTCA
VEGF	AGATGACAGCCAGACAGACAG	CCACAGACTCCCTGCTTTTAC
β-Actin	GCTGTGTTGTCCCTGTATGC	GAGCGCGTAACCCTCATAGA

IL-1β interleukin-1 beta, *IL-6,* interleukin-6, *TNF-α* tumor necrosis factor alpha, *SOD1* superoxide dismutase 1, *TGF-β1* transforming growth factor beta 1, *FGF-2* fibroblast growth factor 2, *COL1α1* collagen type 1 alpha 1, *HGF* hepatocyte growth factor, *HIF-1α* hypoxia-inducible factor-1 alpha, *VEGF* vascular endothelial growth factor, *β-actin* beta actin

Table 2. List of primary and secondary antibodies used in the study

Antibodies	Dilution	Description
Anti-β-actin	1:1000	Mouse monoclonal, Santa Cruz, USA, sc-47 778
Anti-IL-1β	1:200	Rabbit polyclonal, Santa Cruz, USA, sc-7884
Anti-IL-6	1:200	Rabbit monoclonal, Abcam, USA, ab-233 706
Anti-TNF-α	1:200	Rabbit monoclonal, Abcam, USA, ab-215 188
Anti-SOD	1:2000	Rabbit polyclonal, Abcam, USA, ab-13 498
Anti-FGF-2	1:200	Rabbit monoclonal, Abcam, USA, ab-208 687
Anti-TGF-β1	1:50000	Rabbit polyclonal, Abcam, USA, ab-66 043
Anti-COL1α1	1:200	Goat polyclonal, Santa Cruz, USA, sc-25 974
Anti-HGF	1:200	Mouse monoclonal, Santa Cruz, USA, sc-374 422
Anti-HIF-1α	1:200	Mouse monoclonal, Santa Cruz, USA, sc-53 546
Anti-VEGF	1:200	Goat polyclonal, Santa Cruz, USA, sc-1836
AP-labeled antibody	1:1000	Goat anti-rabbit IgG-AP, Abcam, USA, ab-6722 Goat anti-mouse IgG-AP, Abcam, USA, ab-6790
HRP-labeled antibody	1:1000	Donkey anti-goat IgG-HRP, Santa Cruz, USA, sc-2020

β-actin beta actin, *IL-1β* interleukin-1 beta, *IL-6,* interleukin-6, *TNF-α* tumor necrosis factor alpha, *SOD* superoxide dismutase, *FGF-2* fibroblast growth factor 2, *TGF-β1* transforming growth factor beta 1, *COL1α1* collagen type 1 alpha 1, *HGF* hepatocyte growth factor, *HIF-1α* hypoxia-inducible factor-1 alpha, *VEGF* vascular endothelial growth factor, *AP* alkaline phosphatase, *HRP* horseradish peroxidase

alkaline phosphatase conjugated antibody. β-Actin was used as loading control. The relative band intensities were quantified using ImageJ software.

Statistical analysis

The quantitative data were analysed using GraphPad Prism 5 software (v.5.0; Graphpaa, San Diego, CA, USA). Comparisons between 2 groups were carried out using Student's unpaired *t*-test while comparisons of more than one group were carried out using analysis of variance (ANOVA) tests, including one-way and two-way ANOVA tests followed by Bonferroni's post hoc test. The Kruskal Wallis test was used for assessment of histological scoring. Data are presented as the mean ± standard deviation.

Results

Injury characterization and burn depth measurement

Histological assessment (Figure 1b) showed that acid infliction resulted in deep partial thickness burns (second degree), extending from the epidermis to the deep dermis (1.45 mm depth). The burn skin showed attenuated epidermis, epidermal basement destruction, a necrotic reticular layer of dermis and coagulative damage to collagen, with preserved adnexa (i.e sebaceous glands, hair follicles with uninjured epithelium) and sparing of subjacent hypodermis and skeletal muscle. However, in normal skin all 3 layers, i.e. epidermis, dermis and hypodermis, are intact and viable.

Isolation and characterization of ASCs

We obtained approximately 5×10^6 cells from 2–4 grams of rat adipose tissue at P3 within 20 days. Phase contrast imaging showed the fibroblast like, spindle shaped morphology of cultured ASCs at P3 (Figure 2a). Immunocytochemistry was performed on ASCs to confirm their MSC phenotypes before and after preconditioning with curcumin. As expected, curcumin preconditioning did not influence the mesenchymal origin of ASCs as these cells showed immuno-expression of CD markers same like naïve ASCs, i.e. positive expression for mesenchymal markers (CD90: naïve

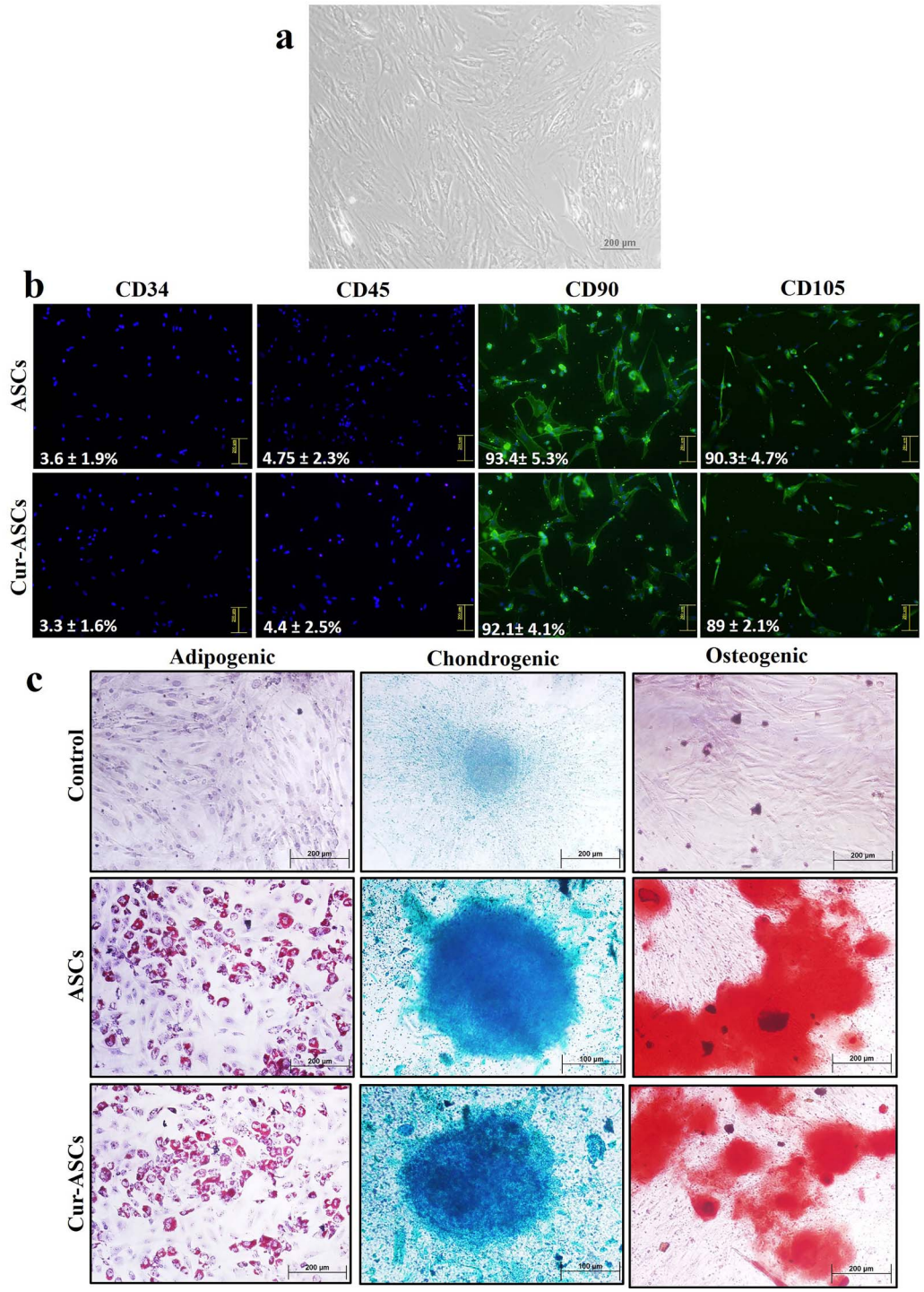

Figure 2. Characterization of adipose-derived mesenchymal stem cells (ASCs). **(a)** Phase contrast microscopy. Spindle shaped morphology of cultured ASCs. Scale bar: 200 µm. **(b)** Immunolabelled fluorescence micrographs of ASCs with and without curcumin preconditioning showing positive expression of cluster of differentiation (CD) 90 and CD105 with negative expression of CD34 and CD45. Magnification: ×200, scale bar: 200 µm. **(c)** Trilineage differentiation potential of ASCs and curcumin preconditions ASCs (Cur-ASCs) compared with control (×200). Adipogenic differentiation demonstrated by intracellular oil droplets stained with oil red O (×200); chondrogenic differentiation demonstrated by Alcian blue staining of glycosaminoglycan deposition (×400); and osteogenic differentiation revealed by Alizarin red staining of calcium deposition (×200)

ASCs, 93.4 ± 5.3%; Cur-ASCs, 92.1 ± 4.1% and CD105, ASCs: 90.3 ± 4.7%; Cur-ASCs: 89 ± 2.1%), and negative expression for endothelial (CD34: naïve ASCs, 3.6 ± 1.9%; Cur-ASCs, 3.3 ± 1.6%) and hematopoietic (CD45: naïve ASCs, 4.75 ± 2.3%; Cur-ASCs, 4.4 ± 2.5%) markers (Figure 2b).

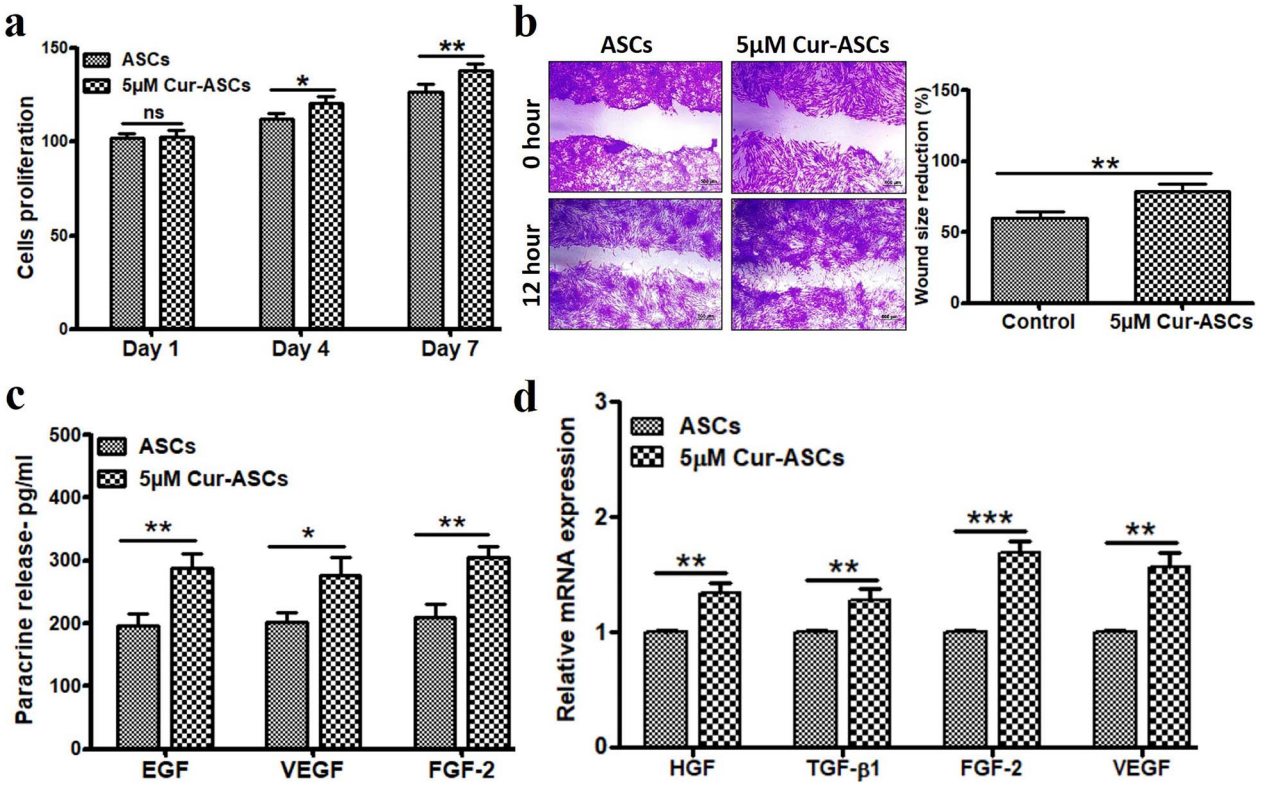

Figure 3. Effects of curcumin preconditioning on proliferation, migration, paracrine release and gene expression regulation in adipose-derived mesenchymal stem cells (ASCs). **(a)** MTT (3-(4, 5-dimethylthiazolyl-2)-2, 5-diphenyltetrazolium bromide) assay showing increased metabolic activity and proliferation potential of ASCs over 7 days in response to 5 μM curcumin dose. **(b)** *In vitro* scratch wound healing assay showing the migration potential of curcumin preconditioned ASCs (Cur-ASCs) *vs* ASCs. Scale bar: 500 μm. **(c)** Quantitative assessment of paracrine release (pg/ml) of epidermal growth factor (EGF), vascular endothelial growth factor (VEGF) and fibroblast growth factor 2 (FGF-2) in Cur-ASCs and ASCs. **(d)** Relative mRNA expression regulation of migratory and healing associated genes, i.e. hepatocyte growth factor (HGF), transforming growth factor beta 1 (TGF-β1), FGF-2 and VEGF in Cur-ASCs *vs* ASCs. Data are presented as mean ± standard deviation. $^{***}p \leq 0.001$, $^{**}p \leq 0.01$, $^{*}p \leq 0.05$ (n = 3). *ns* no significance

In addition, the trilineage differentiation capacity of ASCs and Cur-ASCs was investigated under *in vitro* conditions. As anticipated, curcumin preconditioning did not affect the adipogenic, chondrogenic and osteogenic differentiation potentials of ASCs. As shown in Figure 2c, both ASCs and Cur-ASCs showed strong oil red O (lipid droplets), Alcian blue (secreted proteoglycans) and Alizarin red (calcium deposition) staining and confirmed the differentiation into adipocytes, chondrocytes and osteocytes, respectively. Conversely, in the control group, no oil droplets, proteoglycan secretion or mineralization of calcium phosphate was observed (Figure 2c).

Effects of curcumin preconditioning on proliferation, migration, paracrine release and gene expression regulation in ASCs

The results depicted in Figure 3a show that curcumin preconditioning triggered the metabolic activity of ASCs and increased their proliferation potential over 7 days. Both ASCs and Cur-ASCs showed an increased proliferation rate with time but Cur-ASCs showed relatively higher proliferation than ASCs at day 4 (120.4 ± 3.95% *vs* 112.3 ± 2.67%) and day 7 (137.9 ± 3.45% *vs* 126.7 ± 3.9%).

An *in vitro* scratch wound healing assay was performed to confirm the effect of curcumin preconditioning on the migration potential of ASCs in comparison to non-preconditioned ASCs. It was found that preconditioning significantly improved the migratory activity of Cur-ASCs as compared to ASCs, as evidenced by the significantly increased percentage of wound size reduction in the Cur-ASCs group in comparison to untreated ASCs (78.99 ± 4.93% *vs* 60.02 ± 4.67%) as shown in Figure 3b.

To confirm the influence of curcumin preconditioning on paracrine release of ASCs, ELISA was performed. As shown in Figure 3c, curcumin preconditioning increased the paracrine potential of Cur-ASCs compared with ASCs, as evidenced by increased release of epidermal growth factor (287.9 ± 22.67 pg/ml *vs* 196.78 ± 18.66 pg/ml), VEGF (277.45 ± 26.98 pg/ml *vs* 202.8 ± 15.50 pg/ml) and fibroblast growth factor-2 (FGF-2) (304.56 ± 18.65 pg/ml *vs* 209.7 ± 20.89 pg/ml).

Moreover, gene expression analysis (Figure 3d) revealed that curcumin treatment upregulated expression of migratory and healing-associated markers in Cur-ASCs compared with non-preconditioned ASCs, i.e. HGF (Cur-ASCs: 1.34 ± 0.083 fold *vs* ASCs: 1.0 ± 0.009 fold), transforming growth factor

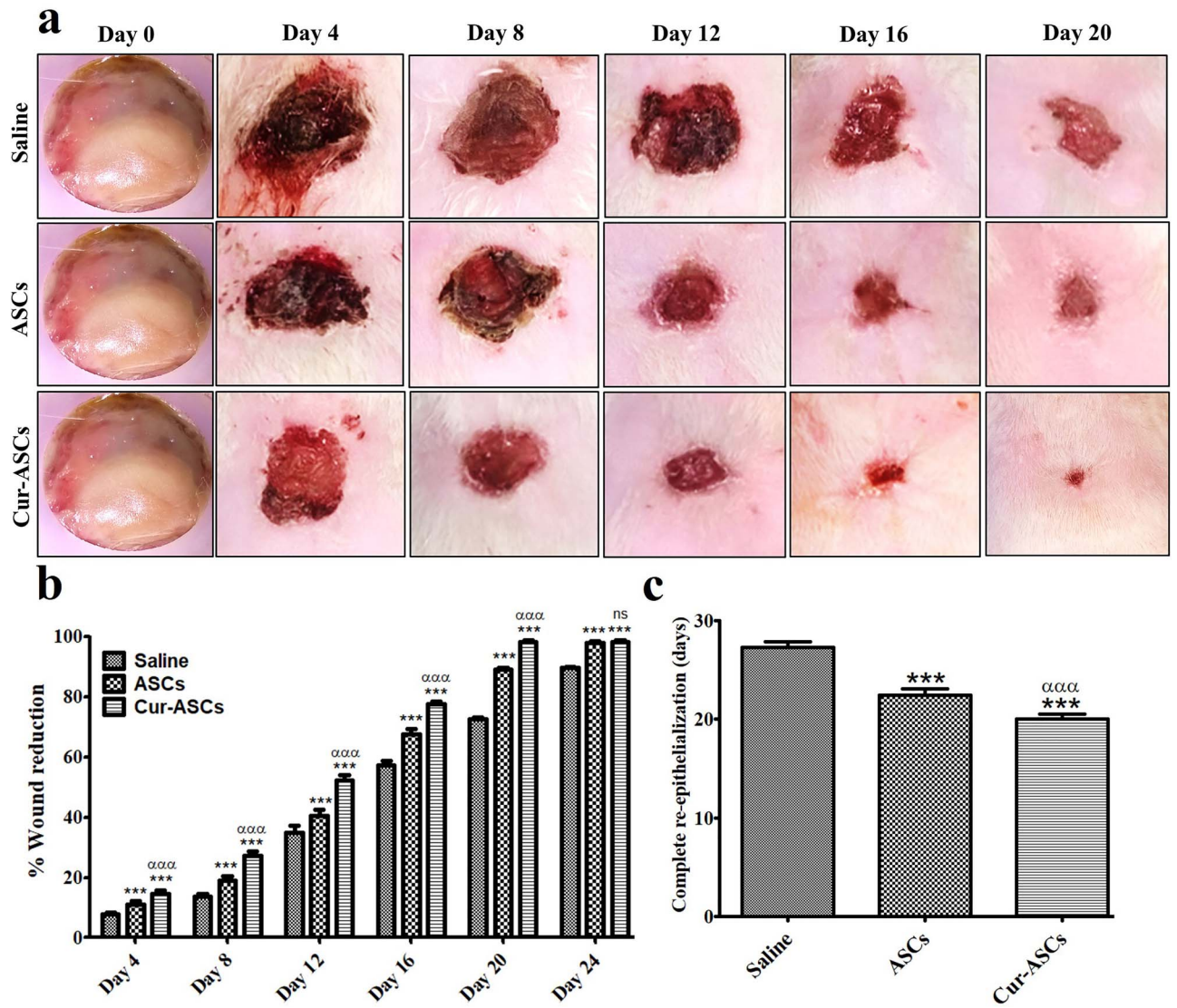

Figure 4. Macroscopic analysis of the wounds treated with ASCs and Cur-ASCs comparative to saline control. **(a)** Representative photographs of wounds at 6 different time points from postoperative days 0, 4, 8, 12, 16 and 20 for each of the following groups: saline, saline injected; ASCs, naïve ASCs injected; Cur-ASCs, curcumin preconditioned ASCs injected. **(b)** Graphical representation of percentage wound size reduction. **(c)** Graphical illustration of period of complete re-epithelization in days. Data are presented as mean ± standard deviation. *denotes saline treated group *vs* ASCs and Cur-ASCs. α denotes ASCs *vs* Cur-ASCs. *** $p \leq 0.001$; $\alpha\alpha\alpha$ $p \leq 0.001$. *ASCs* adipose-derived mesenchymal stem cells, *Cur-ASCs* curcumin preconditioned adipose-derived mesenchymal stem cells

beta 1 (TGF-β1) (Cur-ASCs: 1.28 ± 0.099 fold *vs* ASCs: 1.0 ± 0.015 fold), FGF-2 (Cur-ASCs: 1.69 ± 0.1 fold *vs* ASCs: 1.0 ± 0.008 fold) and VEGF (Cur-ASCs: 1.56 ± 0.13 fold *vs* ASCs: 1.0 ± 0.011 fold).

Effect of Cur-ASCs on healing rate of acid burn wounds

The Cur-ASC treated group tended towards faster wound closure beginning at day 4 and exhibited significantly enhanced wound reduction comparative to ASCs and saline injected controls until day 20 (Figure 4). Wounds of all experimental rats were assessed macroscopically by photography. Figure 4a shows representative gross images of wounds at days 0 (transplantation day), 4, 8, 12 and 16 until the day when the burn wounds of first group were healed (day 20). It was noted that acid burns in the control rats were slow to heal (72.54% wound reduction at day 20); nevertheless, ASC treated rats exhibited comparatively better recovery than those in the saline control group but wounds were still present (89% wound reduction at day 20). However, transplantation of Cur-ASCs significantly improved the healing response and the rats treated with Cur-ASCs had healed completely by day 20. Overall, assessment of wound closure percentage demonstrated that the wound recovery rate was significantly faster in Cur-ASC treated rats than those treated with ASCs or saline control, as shown in Figure 4b. Moreover, earlier re-epithelization was observed in Cur-ASC treated rats (20.0 ± 0.5 days) compared with those treated with ASCs (22.45 ± 0.63 days) or saline (27.33 ± 0.51 days) (Figure 4c). Collectively, these findings demonstrated that Cur-ASC treated rats healed 1.12 times faster (re-epithelization time for ASC treated rats/re-epithelization time for Cur-ASC treated

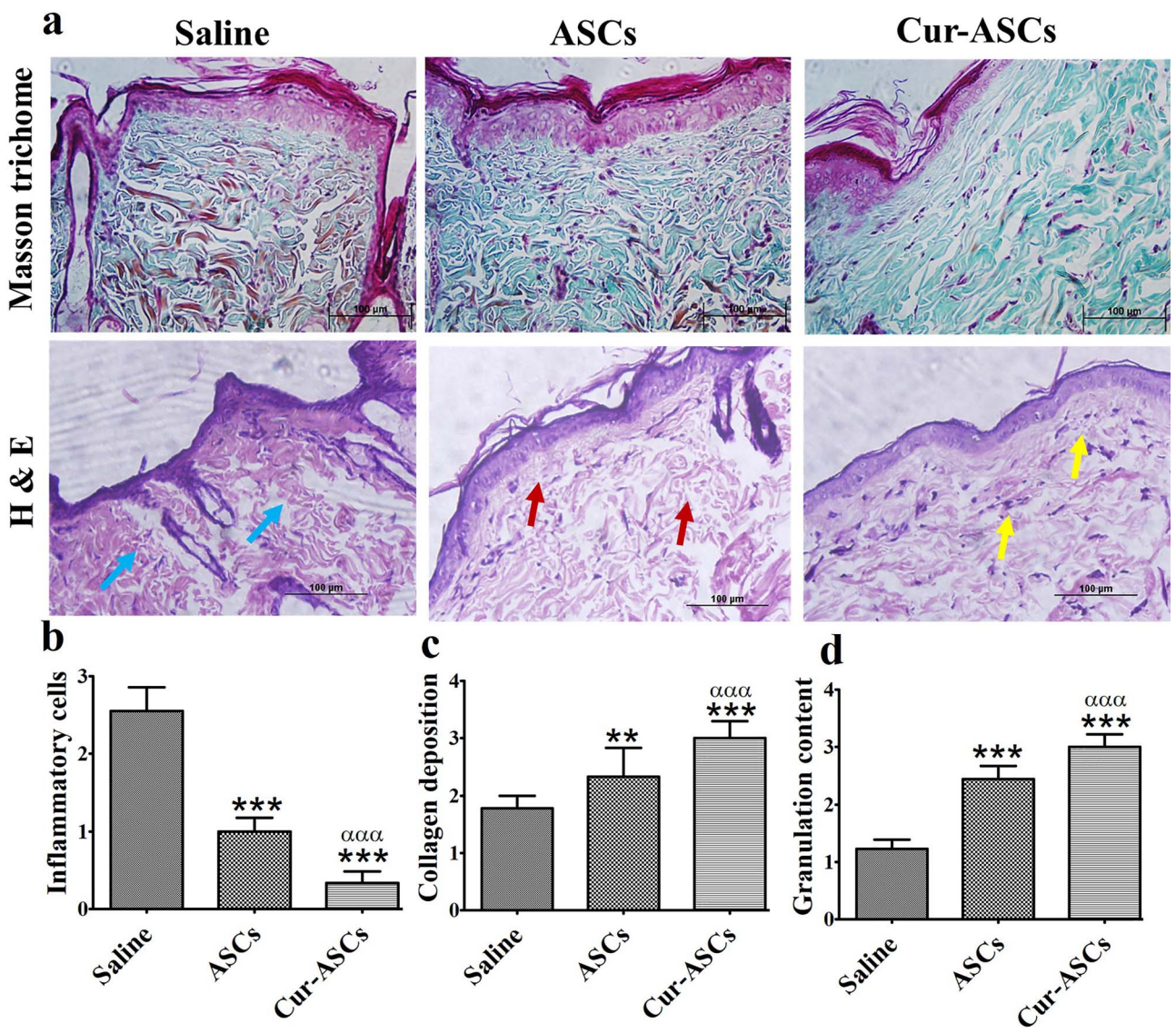

Figure 5. Histological evaluation of healed skin sections harvested 20 days post-wounding. **(a)** Representative images of healed skin stained with Masson's trichrome and hematoxylin and eosin (H&E) at ×400 magnification; scale bar: 100 µm. H&E sections were blind scored (0–3) by a pathologist for inflammatory cells (blue arrows), collagen fibers with dermis (red arrows) and fibroblasts (yellow arrows) from 5 different ×400 power field images per group captured at 10 randomly selected areas. **(b–d)** Graphical representation of statistically analysed histological scores (Kruskal Wallis test) for **(b)** inflammatory cells, **(c)** collagen deposition and **(d)** granulation content. Data are presented as mean ± standard deviation. *denotes saline treated group *vs* ASCs and Cur-ASCs. α denotes ASCs *vs* Cur-ASCs. $^{**}p \leq 0.01$, $^{***}p \leq 0.001$; $\alpha\alpha\alpha$ $p \leq 0.001$. *ASCs* adipose-derived mesenchymal stem cells, *Cur-ASCs* curcumin preconditioned adipose-derived mesenchymal stem cells

rats) than those treated with ASCs and 1.36 times quicker (re-epithelization time for saline treated rats/re-epithelization time for Cur-ASC treated rats) than saline treated rats. This verified that curcumin preconditioning of ASCs enhances their therapeutic efficacy and substantiates them for the healing of challenging acid burn wounds.

Cur-ASCs suppressed wound inflammation and promoted collagen deposition and granulation tissue formation

H&E stained images (Figure 5a) revealed that Cur-ASCs treatment significantly improved the epidermis and dermis architecture upon healing than naïve ASCs and saline treatment. High inflammation is the key factor that impedes the recovery rate and epithelization of burn wounds. Histological scoring demonstrated a marked reduction in infiltration of inflammatory cells, along with significant collagen deposition and pronounced granulation in the excised healed skin of Cur-ASC treated rats compared with ASC and saline control rats (Figure 5b, c, d). Additionally, Masson's trichome staining (Figure 5a) showed the high collagen synthesis (green color) in healed skin in Cur-ASC treated rats compared with ASC and saline control rats.

Cur-ASCs administration resulted in elevated switch from pro-inflammatory status to pro-healing status

Next, we investigated the effect of Cur-ASCs on the regulation of pro-inflammatory cytokines (interleukin-1 beta (IL-1β),

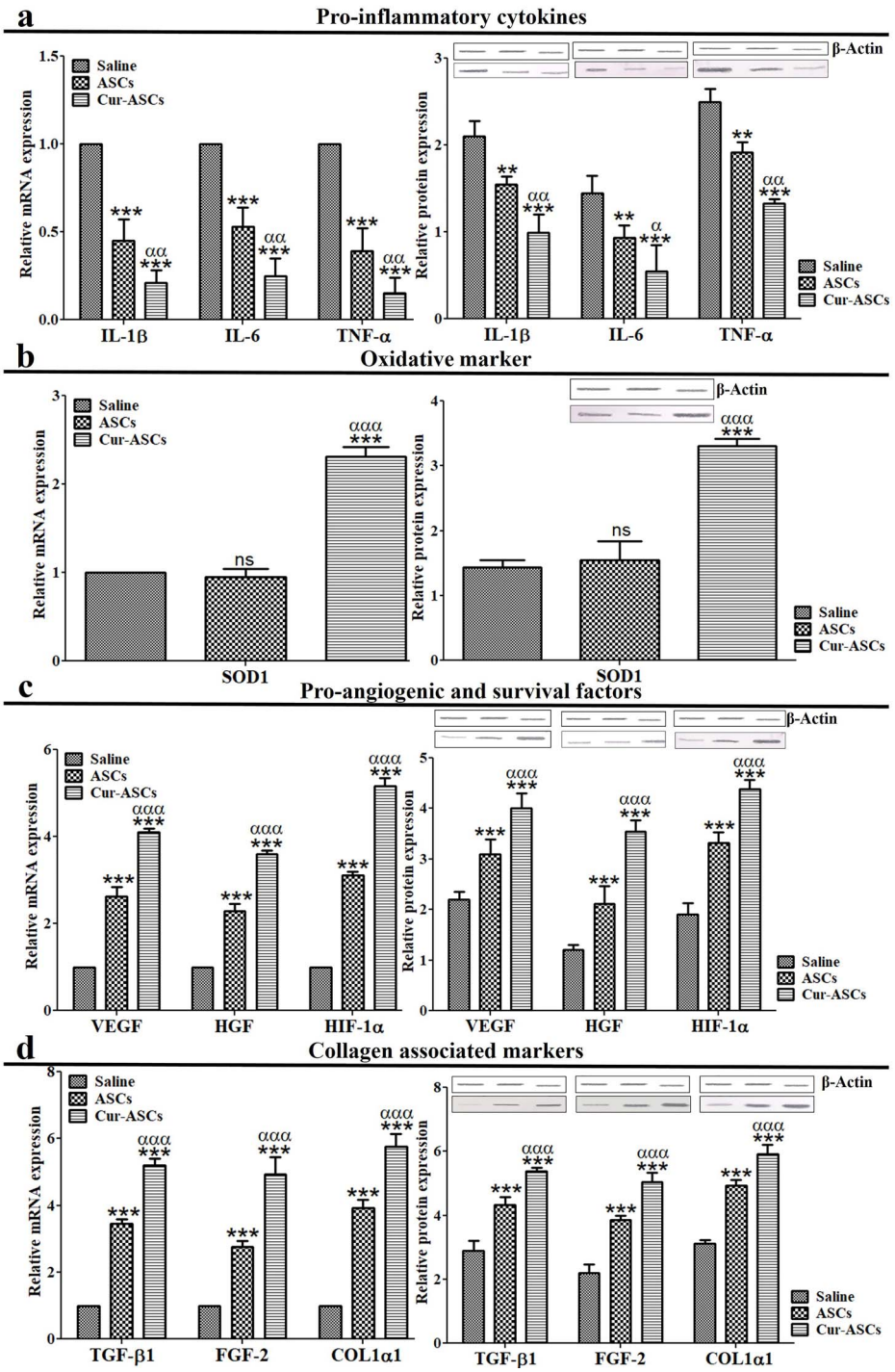

Figure 6. Molecular (gene and protein expression) analysis of wound healing markers by real-time PCR and western blotting. Relative mRNA expression (fold change) and quantitative measurement of relative protein expression (arbitrary unit) of **(a)** pro-inflammatory cytokines, i.e. interleukin-1 beta (IL-1β), interleukin-6 (IL6) and tumor necrosis factor alpha (TNF-α); **(b)** Oxidative marker, i.e. superoxide dismutase 1 (SOD1); **(c)** pro-angiogenic factors, i.e. vascular endothelial growth factor (VEGF), hepatocyte growth factor (HGF) and hypoxia-inducible factor-1 alpha (HIF-1α); and **(d)** collagen content markers, i.e. transforming growth factor beta 1 (TGF-β1), fibroblast growth factor 2 (FGF-2) and collagen type 1 alpha 1 (COL1α1). Values are expressed as mean ± standard deviation (n = 6). *denotes saline treated group *vs* ASCs and Cur-ASCs. α denotes ASCs *vs* Cur-ASCs. $^{**}p \leq 0.01$, $^{***}p \leq 0.001$; $\alpha p \leq 0.05$, $\alpha\alpha p \leq 0.01$, $\alpha\alpha\alpha p \leq 0.001$. *ASCs* adipose-derived mesenchymal stem cells, *Cur-ASCs* curcumin preconditioned adipose-derived mesenchymal stem cells, *ns* no significance

interleukin-6 (IL-6), tumor necrosis factor alpha (TNF-α)) and healing promoters, i.e. an oxidative marker (superoxide dismutase 1 (SOD1)), pro-angiogenic factors (VEGF, HGF, hypoxia-inducible factor-1 alpha (HIF-1α)) and collagen

deposition associated markers (FGF-2, collagen type 1 alpha 1 (COL1α1), TGF-β1) at the molecular level. It was found that Cur-ASC treatment significantly reduced the mRNA and protein expressions of IL-1β (Cur-ASCs: 0.21 ± 0.07 fold and 0.99 ± 0.21 IL-1β/β-actin ratio *vs* ASCs: 0.45 ± 0.12 fold and 1.55 ± 0.09 IL-1/β-actin ratio); IL-6 (Cur-ASCs: 0.25 ± 0.10 fold and 0.55 ± 0.30 IL-1/β-actin ratio *vs* ASCs: 0.53 ± 0.11 fold and 0.93 ± 0.15 IL-1/β-actin ratio); and TNF-α (Cur-ASCs: 0.15 ± 0.09 fold and 1.33 ± 0.05 TNF-α/β-actin ratio *vs* ASCs: 0.39 ± 0.13 fold and 1.92 ± 0.11 TNF-α/β-actin ratio), as shown in Figure 6a. SOD1 expression (Figure 6b) was noticeably upregulated in healed skin from the Cur-ASC group (2.31 ± 0.11 fold and 3.31 ± 0.11 SOD1/β-actin ratio) compared with the ASC group (0.95 ± 0.09 fold and 1.55 ± 0.29 SOD1/β-actin ratio).

Further, Cur-ASC treatment markedly raised the expression of VEGF (Cur-ASCs: 4.11 ± 0.07 fold and 4.0 ± 0.30 VEGF/β-actin ratio *vs* ASCs: 2.62 ± 0.22 fold and 3.1 ± 0.29 VEGF/β-actin ratio); HGF (Cur-ASCs: 3.59 ± 0.10 fold and 3.54 ± 0.23 HGF/β-actin ratio *vs* ASCs: 2.29 ± 0.16 fold and 2.11 ± 0.36 HGF/β-actin ratio); and HIF-1α (Cur-ASCs: 5.16 ± 0.18 fold and 4.39 ± 0.18 HIF-1α/β-actin ratio *vs* ASCs: 3.11 ± 0.09 fold and 3.32 ± 0.21 HIF-1α/β-actin ratio), as shown in Figure 6c. Moreover, pronounced upregulation was observed in the Cur-ASC treated group for TGF-β1 (Cur-ASCs: 5.21 ± 0.20 fold and 5.39 ± 0.11 TGF-β1/β-actin ratio *vs* ASCs: 3.45 ± 0.14 fold and 4.33 ± 0.24 TGF-β1/β-actin ratio); FGF-2 (Cur-ASCs: 4.94 ± 0.50 fold and 5.04 ± 0.30 FGF-2/β-actin ratio *vs* ASCs: 2.75 ± 0.18 fold and 3.85 ± 0.13 FGF-2/β-actin ratio); and COL1α1 (Cur-ASCs: 5.75 ± 0.39 fold and 5.92 ± 0.29 COL1α1/β-actin ratio *vs* ASCs: 3.93 ± 0.24 fold and 4.93 ± 0.17 COL1α1/β-actin ratio), as shown in Figure 6d.

Discussion

In this study, ASCs were characterized with and without curcumin preconditioning as per minimal criteria set for MSCs by the International Society for Cellular Therapy, i.e. plastic adherent; must express mesenchymal surface markers that include CD90, CD105, CD73, CD44 and CD166 without the expression of hematopoietic/endothelial cell surface markers CD34 and CD45; and should have trilineage (adipogenic, chondrogenic, osteogenic) differentiation capacity. Both ASCs and Cur-ASCs were plastic adherent, showed positive expression for CD 90 and CD105 with no expression for CD34 or CD45 and differentiated into adipocytes, chondrocytes and osteocytes. Moreover, curcumin preconditioning enhanced the metabolic activity, migration potential and paracrine release of ASCs and upregulated the expression of important migratory and healing factors.

The current study follows the recent work from our group [31] that showed that curcumin preconditioning augments the therapeutic efficacy of ASCs for efficient healing of diabetic wounds. This finding encouraged us to investigate the competence of Cur-ASCs for the healing of acid inflicted burns. Thus, in this research, acid inflicted burns were enacted in rats to investigate the regenerative effects of Cur-ASCs in terms of better wound healing. The study outcomes were examined through visual inspection, planimetric evaluation, histological assessment and analysis of regulation of healing markers, both at the gene and protein levels. Here, our results demonstrated that Cur-ASCs were superior to naïve ASCs in accelerating re-epithelialization and the closure rate of acid inflicted burn wounds. In addition, localized administration of Cur-ASCs suppressed the inflammatory response, increased angiogenesis and improved granulation and collagen deposition.

MSC-based therapies are gaining hopes for the treatment of hard-to-heal chronic wounds [35] such as chemical burns. Several studies have confirmed that MSC transplantation expedites wound healing and it is believed that the principal mechanism of action of MSCs is through secretory factors that affect the biological functions of surrounding skin cells [36,37]. However, the magnitude of these therapeutic effects after transplantation is highly inconsistent and not enduring. In the majority of cases, these uncertain outcomes have been attributable to the poor survival of transplanted MSCs in the target tissue [38]. However, if even a small proportion of transplanted MSCs are able to remain in the injurious tissue, they are capable of exerting some remedial effects. Based on these premises, it is speculated that if a small percentage of viable MSCs can produce such beneficial effects, then enhancing MSC survival is critical for the clinical efficacy of MSC-based therapies. Recent studies have demonstrated that curcumin considerably enhances the potency of MSCs in various injuries, in that it stimulates proliferation, inhibits apoptosis and increases paracrine secretion, suggesting that pretreatment of MSCs with curcumin may be a promising strategy to further improve their efficacy for tissue repair [39–42]. Thus, we hypothesized that preconditioning of ASCs with curcumin may improve their tolerance to the hostile niche of acid burns, thereby enhancing their therapeutic potential for wound healing, as we have observed in diabetic wounds.

In this study, visual and planimetric evaluation showed that treatment with Cur-ASCs resulted in faster re-epithelialization of acid inflicted burns compared with treatment with naïve ASCs (1.12 times) and the control (1.36 times). This substantial difference in re-epithelialization time built our confidence to suggest the clinical utility of Cur-ASCs in hard-to-heal acidic burn wounds. However, it is worthy to mention that the recovery of 2×2 cm acidic wound in rats model by one-time 2×10^6 Cur-ASCs transplantation is not enough evidence. Since the immune environment and cell dose requirement may substantially differ in larger animals and may present a different outcome, it is recommended to assess the therapeutic effects of Cur-ASCs in relatively higher animals to better represent the clinical efficacy of Cur-ASCs.

The critical challenge to translate stem cell-based therapies into clinic includes immediate availability of cells upon demand at the point of care. For example, for the treatment

of burns, ASCs administration should be performed within a week or at earliest of injury. In recent past, the preconditioning of stem cells has become a more rational approach in terms of clinical feasibility because it could be done in a short time and without high personnel dependency. As in our study, only 24 hours of exposure to curcumin-supplemented medium for cell conditioning is required prior to transplantation. Moreover, reported studies have stated that the preconditioning strategy improved therapeutic efficacy of the cells by supporting their survival, engraftment and paracrine abilities [43–45]. Similarly, we also observed improved therapeutic potential of Cur-ASCs in terms of faster wound recovery in Cur-ASC treated rats compared with ASCs; however, we did not trace the transplanted ASCs at the wound site with regard to their viability, placement and mechanistic role in wound healing. Considering the outcomes of previous reports, it could be speculated that improved wound healing in Cur-ASC treated rats could be attributed to improvement in ASC survival and might be correlated with increased production of secretory factors for a longer period of time, resulting in faster healing.

Inflammatory cell infiltration is an important phase of wound repair [46]; however, its prolonged persistence in the wound bed increases the burden of neutrophils and apoptotic cells through pro-inflammatory cytokines, which ultimately impedes the healing process [47]. Studies have shown that the balance between pro- and anti-inflammatory cytokines is disturbed in non-healing wounds [48]. Our results were also in agreement, as we observed a high number of inflammatory cells in control rats that showed delays in healing. Apart from histological analysis, we noticed high expression of pro-inflammatory cytokines, including Il-1β, Il-6 and TNF-α in control rats. Interestingly, after cell transplantation, Cur-ASC treated rats showed a significant depletion of inflammatory cells in comparison with naïve ASCs. Concomitantly, data assimilated from expressional studies indicated a substantial decrease in the expression of pro-inflammatory cytokines in healed skin from Cur-ASC treated acid burn wounds. It is of note that MSCs have an intrinsic ability to reduce inflammation, as reported in several studies [49–51]; however, the observed substantial decrease in the inflammatory phase might be because of enhanced retention of Cur-ASCs in the wound tissue.

Together with the persistent inflammatory phase, the oxidative microenvironment was also observed in non-healing wounds [52]. It has been demonstrated that the prolonged presence of inflammatory cells in the wound bed produces various reactive radicals, which contributes to oxidative imbalance and further negatively regulates the healing process [53,54]. Superoxide dismutase, an antioxidant enzyme encoded by the Sod1 gene, is a scavenger of reactive radicals and known to protect cells from oxidative damage [55,56]. We did not see any change in Sod1 expression in the naïve ASC treated group compared with the control group. Conversely, higher expression was noticed in the Cur-ASC treated group, which indicates that curcumin preconditioning elicited the ASCs, as well as surrounding cells after transplantation, to neutralize reactive species by deploying antioxidant enzymes. This observation is in line with previous reports which showed that curcumin preconditioning enhances the antioxidant defense potential of MSCs [57,58].

Poor angiogenesis is another hallmark of burns that hampers the wound repair process [59]. MSCs are known to induce angiogenesis upon transplantation via paracrine secretions [60]. Corroborating previous reports [61–63], in this study we observed marked expressions of pro-angiogenic growth factors, such as VEGF, HGF, and HIF-1α, in the Cur-ASC treated group at the molecular level. These findings are in accordance with our previous outcome that Cur-ASC transplantation leads to improved microcirculation in the wound bed of diabetic rats.

TGF-β1 has been shown to play a role in the transformation of fibroblasts into myofibroblasts, which leads to the production of collagen and thereby accelerates the healing of wounds [64,65]. For this reason, we analysed TGF-β1, FGF-2 and COL1α1 expression in our study. As expected, we noticed an increased expression of these genes in the healed skin of the Cur-ASC treated group. This observation was supported by the histological aspects of healed skin, as demonstrated by H&E and Masson's trichrome staining, which revealed much superior granulation tissue with marked fibroblast proliferation and collagen deposition in Cur-ASC treated healed wounds. Previously, enhanced expressions of TGF-β1, FGF-2 and COL1α1 have been observed in healed skin [31,66].

Conclusions

In conclusion, our findings demonstrate that preconditioning of ASCs with curcumin contributes to the efficacy of transplanted ASCs in, and their tolerance to, the hostile niche of acid inflicted burns. Cur-ASCs secreted growth factors for a longer time and resulted in faster healing. Thus, the outcomes of this study suggest the potential clinical utility of Cur-ASCs for the treatment of acid burn wounds and their feasibility for this.

Abbreviations

ASCs: adipose-derived mesenchymal stem cells; CD: cluster of differentiation; COL1α1: collagen type 1 alpha 1; Cur-ASCs: curcumin preconditioned adipose-derived mesenchymal stem cells; DMEM-LG: Dulbecco's Modified Eagle Medium; FBS: fetal bovine serum; FGF-2: fibroblast growth factor 2; H&E: hematoxylin and eosin; HGF: hepatocyte growth factor; HIF-1α: hypoxia-inducible factor-1 alpha; IL-1β: interleukin-1 beta; IL-6: interleukin-6; MSCs: mesenchymal stem cells; P3: passage 3; PBS: phosphate buffered saline; SOD1: superoxide dismutase 1; TGF-β1: transforming growth factor beta 1; TNF-α: tumor necrosis factor alpha; VEGF: vascular endothelial growth factor.

Funding

This work was financially supported by research grants from the Higher Education Commission of Pakistan.

Availability of data and materials

Data and materials related to this work are available from the corresponding author upon request.

Authors' contributions

MA and HG contributed to the study design, experiment conduct, interpretation and analysis of the data and manuscript preparation. HB contributed toward study design and data analysis. RA, AMI and MRA contributed in data analysis. AM and SR contributed with their supervision and critical revision of manuscript. All authors read and approved the manuscript.

Ethics approval and consent to participate

All experimental procedures were approved by the Committee of Animal Care, National Center of Excellence in Molecular Biology, University of the Punjab, Lahore, Pakistan.

Conflicts of interest

None declared.

References

1. Stokes M, Johnson W. Burns in the third world: an unmet need. *Ann Burns Fire Disasters*. 2017;30:243–246.
2. Hardwicke J, Hunter T, Staruch R, Moiemen N. Chemical burns–an historical comparison and review of the literature. *Burns*. 2012;38:383–7.
3. Das KK, Olga L, Peck M, Morselli PG, Salek A. Management of acid burns: experience from Bangladesh. *Burns*. 2015;41:484–92.
4. Blais M, Parenteau-Bareil R, Cadau S, Berthod F. Concise review: tissue-engineered skin and nerve regeneration in burn treatment. *Stem Cells Transl Med*. 2013;2:545–51.
5. Solberg K. Pakistan moves to tackle acid violence. *The Lancet*. 2010;376:1209–10.
6. Holm JS, Toyserkani NM, Sorensen JA. Adipose-derived stem cells for treatment of chronic ulcers: current status. *Stem Cell Res Ther*. 2018;9:142. doi: 10.1186/s13287-018-0887-0.
7. Hu MS, Borrelli MR, Lorenz HP, Longaker MT, Wan DC. Mesenchymal stromal cells and cutaneous wound healing: a comprehensive review of the background, role, and therapeutic potential. *Stem Cells Int*. 2018;2018. doi: 10.1155/2018/6901983.
8. Huang Y-Z, Gou M, Da L-C, Zhang W-Q, Xie H-Q. Mesenchymal stem cells for chronic wound healing: current status of preclinical and clinical studies. *Tissue Eng Part B Rev*. 2020. doi: 10.1089/ten.TEB.2019.0351.
9. Stoltz J-F, de Isla N, Li Y, Bensoussan D, Zhang L, Huselstein C, *et al*. Stem cells and regenerative medicine: myth or reality of the 21th century. *Stem Cells Int*. 2015;2015. doi: 10.1155/2015/734731.
10. Mazini L, Rochette L, Amine M, Malka G. Regenerative capacity of adipose derived stem cells (ADSCs), comparison with mesenchymal stem cells (MSCs). *Int J Mol Sci*. 2019;20:2523. doi: 10.3390/ijms20102523.
11. Oberringer M, Bubel M, Jennewein M, Guthörl S, Morsch T, Bachmann S, *et al*. The role of adipose-derived stem cells in a self-organizing 3D model with regard to human soft tissue healing. *Mol Cell Biochem*. 2018;445:195–210.
12. Hassan WU, Greiser U, Wang W. Role of adipose-derived stem cells in wound healing. *Wound Repair Regen*. 2014;22:313–25.
13. Conese M, Annacontini L, Carbone A, Beccia E, Cecchino LR, Parisi D, *et al*. The role of adipose-derived stem cells, dermal regenerative templates, and platelet-rich plasma in tissue engineering-based treatments of chronic skin wounds. *Stem Cells Int*. 2020;2020. doi: 10.1155/2020/7056261.
14. Kuo Y-R, Wang C-T, Cheng J-T, Kao G-S, Chiang Y-C, Wang C-J. Adipose-derived stem cells accelerate diabetic wound healing through the induction of autocrine and paracrine effects. *Cell Transplant*. 2016;25:71–81.
15. Irons RF, Cahill KW, Rattigan DA, Marcotte JH, Fromer MW, Chang S, *et al*. Acceleration of diabetic wound healing with adipose-derived stem cells, endothelial-differentiated stem cells, and topical conditioned medium therapy in a swine model. *J Vasc Surg*. 2018;68:115S–25.
16. Kosaraju R, Rennert RC, Maan ZN, Duscher D, Barrera J, Whittam AJ, *et al*. Adipose-derived stem cell-seeded hydrogels increase endogenous progenitor cell recruitment and neovascularization in wounds. *Tissue Eng Part A*. 2016;22:295–305.
17. Li P, Guo X. A review: therapeutic potential of adipose-derived stem cells in cutaneous wound healing and regeneration. *Stem Cell Res Ther*. 2018;9:302. https://doi.org/10.1186/s13287-018-1044-5.
18. Zhao L, Hu C, Zhang P, Jiang H, Chen J. Novel preconditioning strategies for enhancing the migratory ability of mesenchymal stem cells in acute kidney injury. *Stem Cell Res Ther*. 2018;9:225. https://doi.org/10.1186/s13287-018-0973-3.
19. Zhao L, Hu C, Han F, Cai F, Wang J, Chen J. Preconditioning is an effective strategy for improving the efficiency of mesenchymal stem cells in kidney transplantation. *Stem Cell Res Ther*. 2020;11:1–11. https://doi.org/10.1186/s13287-020-01721-8.
20. Srifa W, Kosaric N, Amorin A, Jadi O, Park Y, Mantri S, *et al*. Cas9-AAV6-engineered human mesenchymal stromal cells improved cutaneous wound healing in diabetic mice. *Nat Commun*. 2020;11:1–14. https://doi.org/10.1038/s41467-020-16065-3.
21. Ariyanti AD, Zhang J, Marcelina O, Nugrahaningrum DA, Wang G, Kasim V, *et al*. Salidroside-pretreated mesenchymal stem cells enhance diabetic wound healing by promoting paracrine function and survival of mesenchymal stem cells under hyperglycemia. *Stem Cells Transl Med*. 2019;8:404–14.
22. Pirmoradi S, Fathi E, Farahzadi R, Pilehvar-Soltanahmadi Y, Zarghami N. Curcumin affects adipose tissue-derived mesenchymal stem cell aging through TERT gene expression. *Drug Res*. 2018;68:213–21.
23. Zhu W, Wu Y, Meng Y-F, Wang J-Y, Xu M, Tao J-J, *et al*. Effect of curcumin on aging retinal pigment epithelial cells. *Drug Des Devel Ther*. 2015;9:5337. doi: 10.2147/DDDT.S84979.
24. Xiao J, Sheng X, Zhang X, Guo M, Ji X. Curcumin protects against myocardial infarction-induced cardiac fibrosis via

SIRT1 activation in vivo and in vitro. *Drug Des Devel Ther*. 2016;10:1267. doi: 10.2147/DDDT.S104925.
25. González-Salazar A, Molina-Jijón E, Correa F, Zarco-Márquez G, Calderón-Oliver M, Tapia E, *et al.* Curcumin protects from cardiac reperfusion damage by attenuation of oxidant stress and mitochondrial dysfunction. *Cardiovasc Toxicol*. 2011;11:357. doi: 10.1007/s12012-011-9128-9.
26. Jain SK, Rains J, Croad J, Larson B, Jones K. Curcumin supplementation lowers TNF-α, IL-6, IL-8, and MCP-1 secretion in high glucose-treated cultured monocytes and blood levels of TNF-α, IL-6, MCP-1, glucose, and glycosylated hemoglobin in diabetic rats. *Antioxid Redox Signal*. 2009;11:241–9.
27. Ke S, Zhang Y, Lan Z, Li S, Zhu W, Liu L. Curcumin protects murine lung mesenchymal stem cells from H2O2 by modulating the Akt/Nrf2/HO-1 pathway. *J Int Med Res*. 2020;48:0300060520910665. doi: 10.1177/0300060520910665.
28. Cremers NA, Lundvig D, Van Dalen S, Schelbergen RF, Van Lent PL, Szarek WA, *et al.* Curcumin-induced heme oxygenase-1 expression prevents H2O2-induced cell death in wild type and heme oxygenase-2 knockout adipose-derived mesenchymal stem cells. *Int J Mol Sci*. 2014;15:17974–99.
29. Xiao Y, Xia J, Wu S, Lv Z, Huang S, Huang H, *et al.* Curcumin inhibits acute vascular inflammation through the activation of heme oxygenase-1. *Oxid Med Cell Longev*. 2018;2018. https://doi.org/10.1155/2018/3295807.
30. Wang N, Wang F, Gao Y, Yin P, Pan C, Liu W, *et al.* Curcumin protects human adipose-derived mesenchymal stem cells against oxidative stress-induced inhibition of osteogenesis. *J Pharmacol Sci*. 2016;132:192–200.
31. Ghufran H, Mehmood A, Azam M, Butt H, Ramzan A, Yousaf MA, *et al.* Curcumin preconditioned human adipose derived stem cells co-transplanted with platelet rich plasma improve wound healing in diabetic rats. *Life Sci*. 2020;257:118091. doi: 10.1016/j.lfs.2020.118091.
32. Baig MT, Ali G, Awan SJ, Shehzad U, Mehmood A, Mohsin S, *et al.* Serum from CCl4-induced acute rat injury model induces differentiation of ADSCs towards hepatic cells and reduces liver fibrosis. *Growth Factors*. 2017;35:144–60.
33. Azam M, Dikici S, Roman S, Mehmood A, Chaudhry AA, U Rehman I, *et al.* Addition of 2-deoxy-d-ribose to clinically used alginate dressings stimulates angiogenesis and accelerates wound healing in diabetic rats. *J Biomater Appl*. 2019;34:463–75.
34. Kulac M, Aktas C, Tulubas F, Uygur R, Kanter M, Erboga M, *et al.* The effects of topical treatment with curcumin on burn wound healing in rats. *J Mol Histol*. 2013;44:83–90.
35. Dehkordi AN, Babaheydari FM, Chehelgerdi M, Dehkordi SR. Skin tissue engineering: wound healing based on stem-cell-based therapeutic strategies. *Stem Cell Res Ther*. 2019;10:111. https://doi.org/10.1186/s13287-019-1212-2.
36. Hocking AM. Mesenchymal stem cell therapy for cutaneous wounds. *Adv Wound Care*. 2012;1:166–71.
37. Coalson E, Bishop E, Liu W, Feng Y, Spezia M, Liu B, *et al.* Stem cell therapy for chronic skin wounds in the era of personalized medicine: from bench to bedside. *Genes Dis*. 2019;6:342–58.
38. Lee S, Choi E, Cha M-J, Hwang K-C. Cell adhesion and long-term survival of transplanted mesenchymal stem cells: a prerequisite for cell therapy. *Oxid Med Cell Longev*. 2015;2015. doi: 10.1155/2015/632902.
39. Ao XX, Huang H. Curcumin protects mesenchymal stem cells against oxidative stress-induced apoptosis via Akt/mTOR/p70S6K pathway. *Int J Clin Exp Pathol*. 2017;10:6655–64.
40. Liu J, Zhu P, Song P, Xiong W, Chen H, Peng W, *et al.* Pretreatment of adipose derived stem cells with curcumin facilitates myocardial recovery via antiapoptosis and angiogenesis. *Stem Cells Int*. 2015;2015. doi: 10.1155/2015/638153.
41. Ruzicka J, Urdzikova LM, Kloudova A, Amin AG, Vallova J, Kubinova S, *et al.* Anti-inflammatory compound curcumin and mesenchymal stem cells in the treatment of spinal cord injury in rats. *Acta Neurobiol Exp*. 2018;78:358–74.
42. Wang Y-L, Liu X-S, Wang S-S, Xue P, Zeng Z-L, Yang X-P, *et al.* Curcumin-activated mesenchymal stem cells derived from human umbilical cord and their effects on MPTP-mouse model of Parkinson's disease: a new biological therapy for Parkinson's disease. *Stem Cells Int*. 2020;2020. doi: 10.1155/2020/4636397.
43. Pasha Z, Wang Y, Sheikh R, Zhang D, Zhao T, Ashraf M. Preconditioning enhances cell survival and differentiation of stem cells during transplantation in infarcted myocardium. *Cardiovasc Res*. 2008;77:134–42.
44. Zhao L, Hu C, Zhang P, Jiang H, Chen J. Preconditioning strategies for improving the survival rate and paracrine ability of mesenchymal stem cells in acute kidney injury. *J Cell Mol Med*. 2019;23:720–30.
45. Guo L, Du J, Yuan D-F, Zhang Y, Zhang S, Zhang H-C, *et al.* Optimal H2O2 preconditioning to improve bone marrow mesenchymal stem cells' engraftment in wound healing. *Stem Cell Res Ther*. 2020;11:1–17. https://doi.org/10.1186/s13287-020-01910-5
46. Delavary BM, van der Veer WM, van Egmond M, Niessen FB, Beelen RH. Macrophages in skin injury and repair. *Immunobiology*. 2011;216:753–62.
47. Khanna S, Biswas S, Shang Y, Collard E, Azad A, Kauh C, *et al.* Macrophage dysfunction impairs resolution of inflammation in the wounds of diabetic mice. *PLoS One*. 2010;5:e9539. doi: 10.1371/journal.pone.0009539.
48. Zhao R, Liang H, Clarke E, Jackson C, Xue M. Inflammation in chronic wounds. *Int J Mol Sci*. 2016;17:2085. doi: 10.3390/ijms17122085.
49. Shi Y, Wang Y, Li Q, Liu K, Hou J, Shao C, *et al.* Immunoregulatory mechanisms of mesenchymal stem and stromal cells in inflammatory diseases. *Nat Rev Nephrol*. 2018;14:493–507.
50. Pedrazza L, Cubillos-Rojas M, de Mesquita FC, Luft C, Cunha AA, Rosa JL, *et al.* Mesenchymal stem cells decrease lung inflammation during sepsis, acting through inhibition of the MAPK pathway. *Stem Cell Res Ther*. 2017;8:1–14. https//:DOI10.1186/s13287-017-0734-8.
51. Coulson-Thomas VJ, Coulson-Thomas YM, Gesteira TF, WWY Kao. Extrinsic and intrinsic mechanisms by which mesenchymal stem cells suppress the immune system. *Ocul Surf*. 2016;14:121–34.
52. Schäfer M, Werner S. Oxidative stress in normal and impaired wound repair. *Pharmacol Res*. 2008;58:165–71.
53. Park N-Y, Lim Y. Short term supplementation of dietary antioxidants selectively regulates the inflammatory responses during early cutaneous wound healing in diabetic mice. *Nutr Metab*. 2011;8:80. doi: 10.1186/1743-7075-8-80.

54. Mittal M, Siddiqui MR, Tran K, Reddy SP, Malik AB. Reactive oxygen species in inflammation and tissue injury. *Antioxid Redox Signal*. 2014;20:1126–67.
55. Lin Z-F, Xu H-B, Wang J-Y, Lin Q, Ruan Z, Liu F-B, *et al*. SIRT5 desuccinylates and activates SOD1 to eliminate ROS. *Biochem Biophys Res Commun*. 2013;441:191–5.
56. Kook MG, Lee S, Shin N, Kong D, Kim D-H, Kim M-S, *et al*. Repeated intramuscular transplantations of hUCB-MSCs improves motor function and survival in the SOD1 G 93 a mice through activation of AMPK. *Sci Rep*. 2020;10:1–13. https://doi.org/10.1038/s41598-020-58221-1.
57. Wang X, Gao J, Wang Y, Zhao B, Zhang Y, Han F, *et al*. Curcumin pretreatment prevents hydrogen peroxide-induced oxidative stress through enhanced mitochondrial function and deactivation of Akt/Erk signaling pathways in rat bone marrow mesenchymal stem cells. *Mol Cell Biochem*. 2018;443:37–45.
58. Tanwar V, Sachdeva J, Golechha M, Kumari S, Arya DS. Curcumin protects rat myocardium against isoproterenol-induced ischemic injury: attenuation of ventricular dysfunction through increased expression of Hsp27 along with strengthening antioxidant defense system. *J Cardiovasc Pharmacol*. 2010;55:377–84.
59. Zhang X, Wei X, Liu L, Marti GP, Ghanamah MS, Arshad MJ, *et al*. Association of increasing burn severity in mice with delayed mobilization of circulating angiogenic cells. *Arch Surg*. 2010;145:259–66.
60. Bussche L, Van de Walle GR. Peripheral blood-derived mesenchymal stromal cells promote angiogenesis via paracrine stimulation of vascular endothelial growth factor secretion in the equine model. *Stem Cells Transl Med*. 2014;3:1514–25.
61. Katare R, Riu F, Rowlinson J, Lewis A, Holden R, Meloni M, *et al*. Perivascular delivery of encapsulated mesenchymal stem cells improves postischemic angiogenesis via paracrine activation of VEGF-A. *Arterioscler Thromb Vasc Biol*. 2013;33:1872–80.
62. Merino-González C, Zuñiga FA, Escudero C, Ormazabal V, Reyes C, Nova-Lamperti E, *et al*. Mesenchymal stem cell-derived extracellular vesicles promote angiogenesis: potential clinical application. *Front Physiol*. 2016;7:24. doi: 10.3389/fphys.2016.00024.
63. Chen J, Gu Z, Wu M, Yang Y, Zhang J, Ou J, *et al*. C-reactive protein can upregulate VEGF expression to promote ADSC-induced angiogenesis by activating HIF-1α via CD64/PI3k/Akt and MAPK/ERK signaling pathways. *Stem Cell Res Ther*. 2016;7:1–13. https//:DOI10.1186/s13287-016-0377-1.
64. Liarte S, Bernabé-García Á, Nicolás FJ. Role of TGF-β in skin chronic wounds: a keratinocyte perspective. *Cell*. 2020;9:306. doi: 10.3390/cells9020306.
65. Lichtman MK, Otero-Vinas M, Falanga V. Transforming growth factor beta (TGF-β) isoforms in wound healing and fibrosis. *Wound Repair Regen*. 2016;24:215–22.
66. Song Q, Klepeis V, Nugent M, Trinkaus-Randall V. TGF-β1 regulates TGF-β1 and FGF-2 mRNA expression during fibroblast wound healing. *Mol Pathol*. 2002;55:164. doi: 10.1136/mp.55.3.164.